Gynecologic Oncology 161 (2021) 838–844

Contents lists available at ScienceDirect

Gynecologic Oncology

journal homepage: www.elsevier.com/locate/ygyno

Using rADioMIcs and machine learning with ultrasonography for the differential diagnosis of myometRiAL tumors (the ADMIRAL pilot study). Radiomics and differential diagnosis of myometrial tumors

V. Chiappa [a,*], M. Interlenghi [b], C. Salvatore [b], F. Bertolina [a], G. Bogani [a], A. Ditto [a], F. Martinelli [a], I. Castiglioni [c,1], F. Raspagliesi [a,1]

[a] Gynecologic Oncology, Fondazione IRCCS Istituto Nazionale Tumori di Milano, Italy
[b] DeepTrace Technologies S.R.L., Milan, Italy
[c] Dipartimento di Fisica G. Occhialini, University of Milan-Bicocca, Milan, Italy

HIGHLIGHTS

- No imaging technique can effectively discriminate between sarcoma and myoma.
- Inadequate surgery in case of occult sarcoma will worsen the patient's prognosis.
- Radiomics allows to correlate radiological images to the tissue pathophysiology.
- Radiomics applied to US images represents an effective diagnostic support tool.

GRAPHICAL ABSTRACT

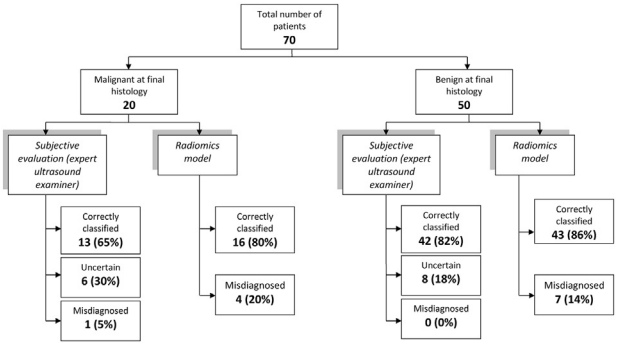

ARTICLE INFO

Article history:
Received 24 December 2020
Accepted 5 April 2021
Available online 16 April 2021

Keywords:
Radiomics
Ultrasound
Uterine sarcoma
Artificial intelligence
Predictive model

ABSTRACT

Objective. To develop and evaluate the performance of a radiomics and machine learning model applied to ultrasound (US) images in predicting the risk of malignancy of a uterine mesenchymal lesion.

Methods. Single-center retrospective evaluation of consecutive patients who underwent surgery for a malignant uterine mesenchymal lesion (sarcoma) and a control group of patients operated on for a benign uterine mesenchymal lesion (myoma). Radiomics was applied to US preoperative images according to the International Biomarker Standardization Initiative guidelines to create, validate and test a classification model for the differential diagnosis of myometrial tumors. The TRACE4 radiomic platform was used thus obtaining a full-automatic radiomic workflow. Definitive histology was considered as gold standard. Accuracy, sensitivity, specificity, AUC and standard deviation of the created classification model were defined.

Results. A total of 70 women with uterine mesenchymal lesions were recruited (20 with histological diagnosis of sarcoma and 50 myomas). Three hundred and nineteen radiomics IBSI-compliant features were extracted and 308 radiomics features were found stable. Different machine learning classifiers were created and the best classification system showed Accuracy 0.85 ± 0.01, Sensitivity 0.80 ± 0.01, Specificity 0.87 ± 0.01, AUC 0.86 ± 0.03.

Conclusions. Radiomics applied to US images shows a great potential in differential diagnosis of mesenchymal tumors, thus representing an interesting decision support tool for the gynecologist oncologist in an area often characterized by uncertainty.

* Corresponding author at: Department of Gynecologic Oncology, Fondazione IRCCS Istituto Nazionale Tumori, Via Venezian 1, 20133 Milan, Italy.
E-mail address: valentina.chiappa@istitutotumori.mi.it (V. Chiappa).
[1] The authors equally contributed to the paper.

https://doi.org/10.1016/j.ygyno.2021.04.004
0090-8258/

1. Introduction

Uterine sarcomas are a rare form of mesenchymal tumors characterized by a poor prognosis; they represent 1% of cancers of the female genital tract and 3–7% of all uterine malignancies [1,2].

In 2014 a Food and Drugs Administration (FDA) safety communication warned against the use of the uterine morcellator during minimally invasive surgery of uterine myomas as it could promote the dissemination of malignant debris in case of an occult malignant lesion [3].

An accurate preoperative diagnosis of myometrial tumors is essential to plan an adequate surgery without the risk of worsening the patient's prognosis in case of uterine sarcoma and minimally invasive so as not to increase the patient's morbidity in case of uterine myoma [4].

The rate of unexpected uterine sarcomas at histological examination described in literature in women undergoing surgery for an apparent benign uterine disease ranged between 0.3 and 1% [5–8].

Unfortunately, the absence of specific symptoms and an imaging that is not always decisive with overlapping characteristics between benign and malignant lesions often do not allow an adequate differential diagnosis between uterine sarcomas and myomas at preoperative workup.

In this scenario, the identification of tools for improving the differential diagnosis represents a current unmet clinical need.

Recently radiomics emerged as a new and encouraging method able to extract and quantify features from radiological medical images [9,10] containing information that reflect the underlying pathophysiology of tissues, such as specific heterogeneity in the shape and texture of lesions [11,12]. The extracted information can be correlated to the clinical data of the patients, in particular to histopathological results, so as to define radiomic biomarker profiles to distinguish malignant tissues from benign ones. Moreover, it is possible to build predictive models using radiomic features to train machine learning systems with the supervision of clinicians in agreement with the histological labels assumed as ground truth [13].

The possibility of relying on a predictive model capable of automatically classifying tissue images represents an interesting and potentially game changer tool for personalized medicine [14], that could be used to improve the diagnostic confidence of clinicians and to stratify the risk at the level of single patients, according to a personalized medicine paradigm.

In the present paper our aim is to test the predictive performance of radiomics-based machine learning models on patients diagnosed with a uterine mesenchymal lesion. For this purpose, we extracted radiomics features from ultrasonographic (US) images of histologically proved uterine sarcomas and myomas and used selected radiomic features to train an ensemble of machine learning systems to develop an automatic predictive model of the risk of malignancy of mesenchymal tumors.

2. Methods

2.1. Study design and study population

This is a single center, retrospective, pilot study.

The study was approved by the local Ethical Committee (Prot. ID INT 155/20, full study protocol available).

We enrolled all consecutive patients treated for a uterine sarcoma at Fondazione IRCCS Istituto Nazionale dei Tumori of Milan from 2015 to 2020 and a control group of consecutive patients diagnosed with a uterine myoma undergoing surgery at the same Institution.

Patients records were found in surgical and pathological registers. Every patient signed written consent for research purpose.

Inclusion criteria were: (i) patients undergoing surgery for myometrial lesion, (ii) execution of a preoperative ultrasound within 6 weeks before surgery, (iii) ultrasound images stored and available for radiomics analysis, (iv) available histologic examination.

2.2. Ultrasonographic images and histology

We retrospectively collected all US images of patients who underwent surgery for uterine sarcoma and a control group of consecutive patients undergoing surgery for uterine myoma.

Images were exported from US machine and stored in .jpg and DICOM (.dcm) format for subsequent analysis. All patients included underwent transvaginal US eventually completed by transabdominal scan in case of big lesions non completely assessable with transvaginal approach or for abdominal staging purpose.

All US examinations were performed at the dedicated ultrasound center of this Institution by two different examiners with more than ten years of experience in the field of gynecological oncological US.

US examinations were performed with the same two US machines (General Electrics Voluson E8 and Samsung Medison Co. HERA w10).

Clinical characteristics of the patients (age, parity, menopausal status and presenting symptoms) and histopathological and US characteristics of the lesions were retrospectively collected and organized in a dedicated Excel File (Microsoft Office Excel 2019 v.17.0, Redmond, WA, USA).

Ultrasound characteristics of the lesions were extracted from original US reports and summarized accordingly to the multicentric consensus study on clinical and ultrasound characteristics of uterine sarcoma [15]. The following US features were recorded in our database: largest diameter of the lesion (mm), number of lesions (single/multiple), visible normal myometrium (Yes/No), type of tumor (Solid/Multilocular-solid) [16], echogenicity of the solid tissue subjectively assessed by the US examiner (Homogenous/Inhomogeneous), presence of cystic areas within the lesion (Yes/No), presence of shadows (No/Internal shadows/Fan shaped shadowing) [17], presence of calcifications (Yes/No), tumor border (Regular/Irregular), Color Score (1/2/3/4) [16], endometrial cavity evaluable (Visible/Not clearly visualized), presence of free fluid in the pouch of Douglas (Yes/No) or ascites (Yes/No).

The subjective impression of the US examiner was also reported and defined as Malignant/Uncertain/Benign lesion.

All patients included in the study underwent surgery (as reported in the inclusion criteria); the type of surgery was tailored on the basis of patients' and lesions' characteristics. In case of uterine sarcoma, the stage of disease was assessed according to the International Federation of Obstetrics and Gynecologists (FIGO) system [18]. Histological subtypes of uterine sarcoma were reported according to the World Health Organization (WHO) classification [19].

In control group, in case of multiple uterine myomas, the lesion with more complex US appearance (bigger and/or colliquated, with inhomogeneous echogenicity, without shadows) was considered for the subsequent radiomics analysis.

2.3. Radiomics study

Radiomics methodology was applied to the collected US images of patients, according to the International Biomarker Standardization Initiative (IBSI) guidelines (https://arxiv.org/abs/1612.07003) [20].

For this purpose, the TRACE4 radiomic platform was used (http://www.deeptracetech.com/files/TechnicalSheet__TRACE4.pdf) allowing the whole IBSI-compliant radiomic workflow to be obtained in a full-automatic way even for US images. IBSI radiomic workflow included: (i) the segmentation of the lesion region from each patient image, (ii) the preprocessing of image content within the segmented region of interest for the radiomic feature extraction, (iii) the extraction of radiomic features from the segmented region of interest, (iv) the selection of radiomic features which remains stable with respect to different segmentations, as may occur by different examiners, and repeatable in test–retest study, (v) the use of such candidate radiomic features to train, validate, and test different systems of machine learning classifiers in the binary classification task of interest (malignant vs benign), by the reduction of such stable and repeatable features to not-redundant

features, in a number that is statistically comparable with the number of collected images of patients.

More specifically:

(i) The segmentations of the myometrial lesions were performed manually, using the TRACE4 segmentation tool and then randomly changed by TRACE4 in order to avoid the dependence of the contour from the segmenter.
(ii) The preprocessing of image intensities within the segmented region of interest included resampling to isotropic voxel spacing, using a down-sampling scheme by considering image slice thickness of 1 mm and intensity discretization using a fixed number of 64 bins.
(iii) The radiomics features extracted from the segmented region of interest belong to different families: morphology, intensity-based statistics, intensity histogram, gray-level co-occurrence matrix (GLCM), gray-level run length matrix (GLRLM), gray-level size zone matrix (GLSZM), neighborhood gray tone difference matrix (NGTDM), gray-level distance zone matrix (GLDZM), neighboring gray level dependence matrix (NGLDM). Their definition, computation and nomenclature are compliant with the IBSI guidelines, except for the features of the family morphology, originally designed for 3D images, which were replaced with ten 2D equivalent features (e.g., 3D features volume and surface were replaced with 2D features area and perimeter, respectively). Steps from (ii) to (iii) was performed using the TRACE4 Radiomics tool. Radiomic features were reported by TRACE4 according to IBSI standards.
(iv) The selection of radiomic features, stable with respect to different segmentations and repeatable in test–retest study, was performed by ICC (ICC > 0.80) by statistically comparing features obtained by data augmentation strategies, (a) generating random variations of the manual segmentation of the lesion region (performed by the operator), and random rotations of the original images and segmentations to reduce the dependency from the operator and to enrich the dataset, respectively. The selected radiomic features (stable and repeatable) were reported by TRACE4.
(v) A different system of machine learning classifier was trained, validated, and tested, for the binary classification task (malignant vs benign, based on histopathology results), reducing the more stable and reproducible features to a signature of not redundant features proper with the number of collected images.

Steps (iv) and (v) were performed automatically by the TRACE4 Modeling and Statistics tool.

The created classification systems were:

1) an ensemble of 10 Support Vector Machines, combined with principal components analysis and fisher discriminant ratio with majority vote rule;
2) an ensemble of 10 Random Forests, combined with Gini index with majority vote rule;
3) an ensemble of 10 kNNs, with majority vote rule;

Nested *K*-fold cross validation method was used, with $K = 10$.

Oversampling technique for the minority class (sarcoma) was applied by adaptive synthetic sampling method.

The predictive performance of the above-described classification systems was measured across the different folds ($K = 10$) in terms of max and mean Accuracy, Sensitivity, Specificity, Area Under the Curve (AUC), Positive Predictive Value (PPV), Negative Predictive Value (NPV), and standard deviation (Confidence Interval, CI, *p*-value [21]).

The study is reported according to STARD guidelines; STARD checklist is available as Supplementary material (1S).

The sample size was calculated according to Hajian-Tilaki analysis for diagnostic studies [22]. We assumed a sensitivity of 85% in predicting malignancy, we selected a 30% prevalence of malignancy in our study population. With a precision of estimate (the maximum marginal error) d = 5%, and a type I error alpha = 0.10, a sample size of 70 patients was needed to test the general hypothesis of the predictive model (to answer whether radiomics predicted malignant versus benign uterine masses).

3. Results

3.1. Ultrasonographic images and histopathological data of patients

We retrospectively enrolled 70 patients with available US images: 20 with definitive histological diagnosis of a uterine sarcoma and 50 patients with benign uterine myomas (control group).

Clinical characteristics of the patients are summarized in Table 1.

Women with uterine sarcomas were significantly older than women with benign myomas, with a median age respectively of 59 and 55 years old.

Most of patients in uterine sarcoma group (75%) were postmenopausal; in the control group 56% of patients were postmenopausal.

Most of patients (70% in sarcoma group, 64% in control group) referred symptoms before US examination and the most common presenting symptom in sarcoma group was abnormal uterine bleeding (40%).

Histopathological characteristics of the malignant myometrial lesions after surgery are summarized in Table 2.

Most of tumors (75%) were leiomyosarcomas and most of cases (50%) were diagnosed in early stage (FIGO stage I).

Ultrasonographic characteristics of the lesions are summarized in Table 3.

Median diameter of the lesion was significantly different between the two groups, with a median diameter respectively of 100 mm (range 43–200 mm) in sarcoma group and 52 mm (range 20–199 mm) in control group.

At US, compared with myomas, uterine sarcomas appeared more frequently as a single solid (90%) mass with inhomogeneous echogenicity (80%), cystic areas (60%), no shadowing (60%), no calcifications (80%) and irregular borders (60%). Fig. 1 summarizes the recurrent US features of myomas and sarcomas.

In all cases of uterine myoma and most cases of malignant tumor (65%), normal myometrium was visible at US.

Vascularization and the presence of ascites or free fluid in the pouch of Douglas were not significantly different between the two groups.

Table 1
Clinical characteristics of the patients. Results are presented as n (%).

Variable	Malignant lesions N = 20	Benign lesions (control group) N = 50	p-Value
Age (median)	59 Range 36–76	55 Range 29–81	<0.001
Nulliparous	4 (20)	27 (54)	0.015
Premenopausal	5 (25)	22 (44)	0.179
Symptoms			
Asymptomatic	6 (30)	17 (34)	0.787
Abnormal vaginal bleeding	8 (40)	7 (14)	0.024
Pelvic or abdominal pain	5 (25)	4 (8)	0.106
Mass detected on other imaging technique	2 (10)	9 (18)	0.493
Self-palpated mass	1 (5)	0 (0)	0.285
Other	1 (5): urinary incontinence	2 (4): dysmenorrhea, infertility	1

Table 2
Histopathological characteristics of the malignant lesions. Results are presented as n (%).

Variable	Malignant myometrial lesions N = 20
Histological type of sarcoma	
Leiomyosarcoma (LMS)	15 (75)
Endometrial stromal sarcoma (ESS)	3 (15)
Undifferentiated endometrial sarcoma (USS)	2 (10)
FIGO stage	
I	10 (50)
II	1 (5)
III	3 (15)
IV	6 (30)

Most of sarcomas (65%) and myomas (82%) were correctly diagnosed respectively as malignant and benign lesions at preoperative US, but a considerable number of lesions have been 'labeled' as uncertain (30% of sarcomas and 18% of myomas) and a sarcoma (5%) was described as a benign lesion by subjective impression of the examiner.

Table 3
Ultrasound characteristics of the benign and malignant myomatrial lesions in the original report. Results are presented as n (%).

Variable	Malignant lesions N = 20	Benign lesions (control group) N = 50	*p*
Largest diameter of the lesion (mm)	100 Range 43–200	52 Range 20–199	***<0.001***
Number of lesions			
Single	18 (90)	28 (56)	*0.010*
Multiple	2 (10)	22 (44)	
Visible normal myometrium			
Yes	13 (65)	50 (100)	***<0.001***
No	7 (35)	0 (0)	
Type of tumor			
Multilocular-solid	2 (10)	1 (2)	*0.194*
Solid	18 (90)	49 (98)	
Echogenicity of solid tissue			
Homogeneous	4 (20)	48 (96)	***<0.001***
Inhomogeneous	16 (80)	2 (4)	
Cystic areas			
Yes	12 (60)	1 (2)	***<0.001***
No	8 (40)	49 (98)	
Shadowing			
No shadowing	12 (60)	12 (24)	
Internal shadows	7 (35)	22 (44)	*0.006*
Fan-shaped shadowing	1 (5)	16 (32)	
Calcifications			
Yes	4 (20)	14 (28)	*0.560*
No	16 (80)	36 (72)	
Tumor border			
Regular	8 (40)	49 (98)	***<0.001***
Irregular	12 (60)	1 (2)	
Color score			
1	1 (5)	25 (50)	
2	4 (20)	18 (36)	*0.003*
3	12 (60)	5 (10)	
4	3 (15)	2 (4)	
Endometrial cavity:			
Visualized	10 (50)	49 (98)	***<0.001***
Not clearly visualized	10 (50)	1 (2)	
Free fluid in the pouch of Douglas			
Yes	4 (20)	0 (0)	*0.005*
No	16 (80)	50 (100)	
Ascites			
Yes	1 (5)	0 (0)	*0.285*
No	19 (95)	50 (100)	
Subjective impression at Ultrasound			
Malignant	13 (65)	0 (0)	***<0.001***
Uncertain (malignancy could not be excluded)	6 (30)	8 (18)	
Benign	1 (5)	42 (82)	

3.2. Radiomics study

Three hundred and nineteen radiomics IBSI-compliant features were extracted from the 70 segmented myometrial lesions, and 308 radiomics features were found stable with respect to different examiners' segmentations and to test-retest study (ICC > 0.8). Table 2S and 3S (Supplementary materials) show, as representative examples, the list of 308 stable radiomic features, their values and nomenclature for a sarcoma and a myoma lesion.

These 308 features were used for the supervised training-validation-testing (nested 10-fold cross validation) of the three ensembles of classifiers, using the histopathological results as labels.

Accuracy, sensitivity, specificity, AUC, PPV and NPV of such classifiers are shown in Table 4.

The best radiomic system was found the ensemble of SVMs. The mean accuracy and AUC of the three best SVMs was good (0.85 ± 0.01, 0.86 ± 0.03), with a good balance between Sensitivity (0.80 ± 0.01) and Specificity (0.87 ± 0.01). To be noted, the NPV was particularly very good (0.92 ± 0.01) at poor cost of PPV (0.73 ± 0.02). These results suggest a high potential of radiomic approach when applied to US images of uterine masses for the differential diagnosis of sarcoma vs myoma.

Fig. 2 shows, as representative graphical examples, the radiomic features "entropy" measured for 3 sarcomas (Fig. 2 a,b,c), and 3 myomas (Fig. 2 d,e,f), respectively. A different level of expression of the entropy can be visually observed from the entropy locally mapped and overlapped to the original corresponding US lesions, for better interpretation of radiomic results.

Fig. 3 shows the flow chart of the study.

4. Discussion

In this study we have demonstrated that radiomics applied to US images can discriminate between uterine sarcomas and myomas with good accuracy, representing a valuable additional tool in the diagnostic workup of these patients.

We considered a series of 20 consecutive patients with a histological diagnosis of uterine sarcoma and a control group of 50 patients with a definitive histological diagnosis of uterine myoma, all undergoing preoperative ultrasound.

We applied radiomics to the exported ultrasound images and used stable radiomics features to create and train a predictive diagnostic machine learning model that showed a predictive accuracy >80%.

Applying radiomics to US images has some advantages with respect to other imaging methods. In fact, US, after clinical evaluation, is the first choice method for investigating myometrial lesions; moreover, US is fast, cheap and allows the examiner assessing the pelvis with good accuracy.

Unfortunately, the clinical evaluation of the patients does not help to discriminate between benign and malignant myometrial lesions, as most of the patients in both groups come to gynecological evaluation presenting some overlapping symptoms; the symptoms reported by our patients are in agreement with what is described in literature [23] and the most frequent symptom in case of uterine sarcoma is abnormal uterine bleeding.

Several studies have described recurrent ultrasound features of uterine sarcomas qualitative observed by the operators: Exacoustos in 2007 [24] suggested that the presence of a single, large, rapidly growing myometrial lesion, with cystic degeneration and with marked peripheral and central vascularization is suggestive of the presence of a uterine leiomyosarcoma. However, unfortunately, these characteristics can also

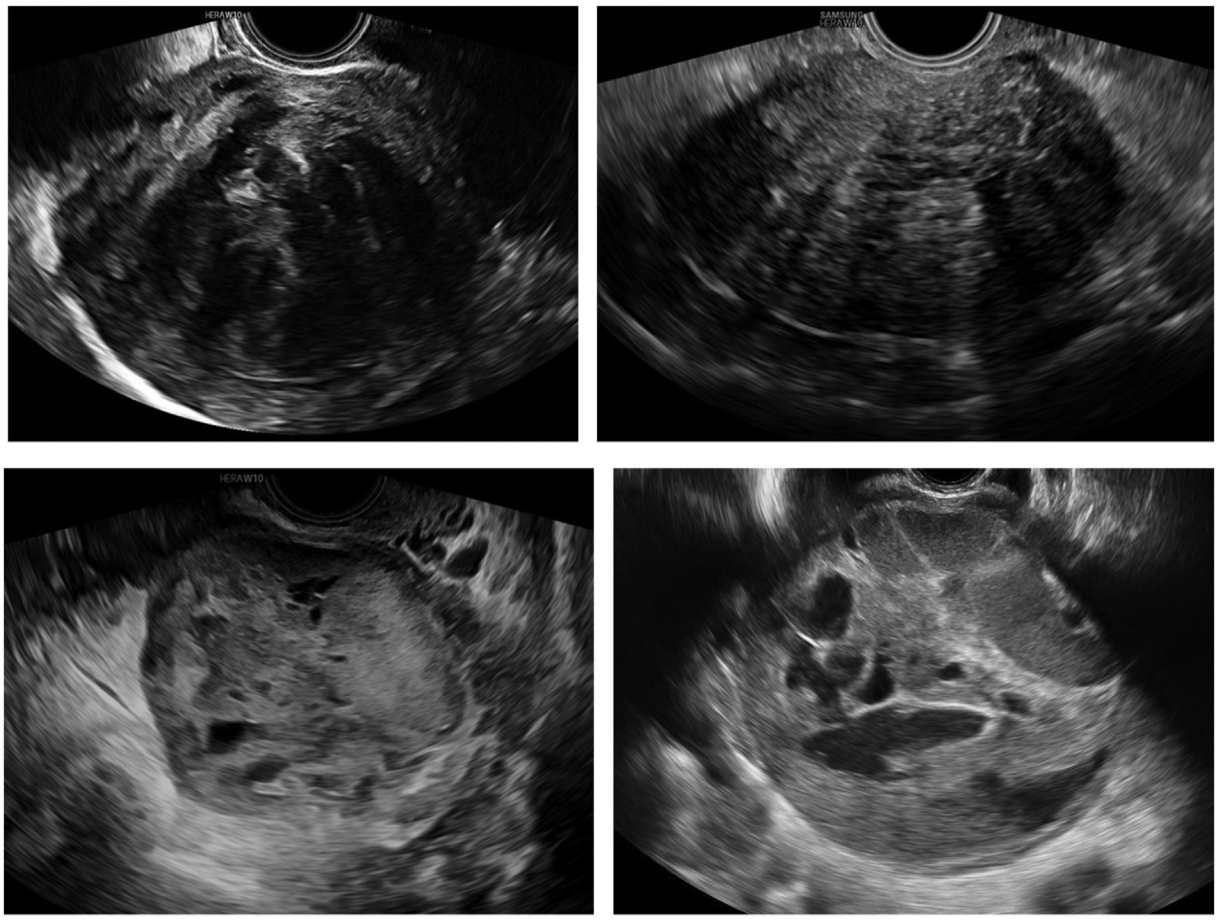

Fig. 1. US recurrent characteristics of uterine mesenchymal tumors: uterine myomas (1A and 1B) are usually solid lesions showing homogeneous echogenicity and shadows; uterine sarcomas (1C and 1D) are solid or multilocular-solid lesions showing inhomogeneous echogenicity, no shadows, irregular cystic areas.

be present in a group of atypical myomas that show cystic, myxoid, red, hydropic or hyaline degeneration.

The presence of internal and fan-shaped shadows is generally associated with benign myometrial lesions (leiomyomas, adenomyosis) [25,26], but in our series they were also present in 40% of uterine sarcomas (and in 76% of patients in the control group).

Moreover, in 2019 Ludovisi [15] described the ultrasound features of uterine sarcomas (dividing them into leiomyosarcomas, endometrial stroma sarcomas, and undifferentiated sarcomas) in the largest series in the literature, concluding that the US features suggestive for malignancy are the presence of a large myometrial lesion, with inhomogeneous echogenicity, with irregular cystic areas, absence of shadows, absence of calcifications in symptomatic women (in particular with abnormal uterine bleeding). In Ludovisi series, after review of the images by a consensus of experts, 36% of patients with uterine sarcoma showed the presence of internal shadows or fan-shaped shadowing.

As proven by all the above-mentioned studies, semantic features are often reported characterizing the size, shape and texture of uterine lesions as observed on US images. Quantifying all these features in a more objective way and considering them in combination in a multivariate model can help to differentiate the groups, and this is what a radiomic machine learning model can provide.

In the paper of Ludovisi et al., the US examiner originally correctly diagnosed only 47% of the lesions as certainly malignant, and suspected malignancy in a further 31% of the lesions, while 21.5% had been misdiagnosed as benign.

In our series, the US examiner correctly classified 65% of sarcomas as malignant, in one case (5% the myometrial tumor was incorrectly classified as benign and a further 30% were uncertain (malignancy couldn't be excluded). In the control group, the US examiner classified no myoma as malignant, but 18% of myomas as uncertain (malignancy couldn't be excluded).

In the uncertain cases, if the US examiner had consulted the radiomic model, he/she would have received a correct malignant answer in 83% respectively, and benign answer in 78% of cases, such results proving a high potential of radiomic model in improving the diagnosis. It should also be noted that the US evaluations in our patient series were all performed by experienced examiners and that among examiners with

Table 4
Performance of the developed radiomic model of sarcoma vs myoma (n = 20 vs 50). 308 stable features among 319 extracted were used as input to the model. Data are expressed as % ± standard deviation [95% CI] and *p* value (* = p-value <0.05, ** = p-value<0.005).

Sarcoma Vs myoma model	Accuracy	Sensitivity	Specificity	AUC	PPV	NPV
Mean from 10 ensembles	0.83 ± 0.03 [80–85]**	0.76 ± 0.05 [72–80]**	0.85 ± 0.03 [83–87]**	0.83 ± 0.04 [80–86]**	0.68 ± 0.05 [62–72]**	0.90 ± 0.02 [88–91]**
Mean from 3 best ensembles	0.85 ± 0.01 [83–87]**	0.80 ± 0.01 [80–80]**	0.87 ± 0.01 [84–90]**	0.86 ± 0.03 [82–91]**	0.73 ± 0.02 [66–75]**	0.92 ± 0.01 [91–92]**

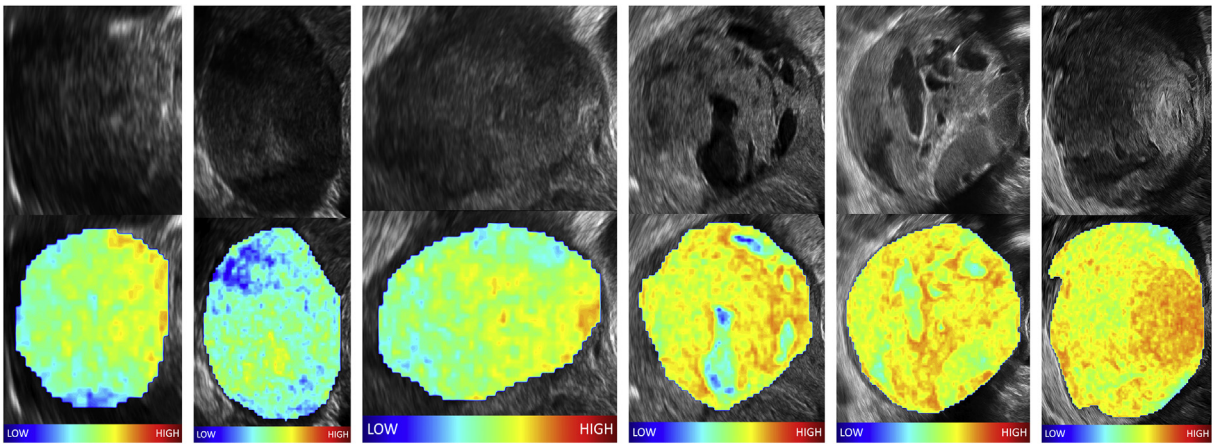

Fig. 2. Local spatial distribution of the feature Entropy evaluated on the Gray-Level Co-occurence Matrices: Sarcoma (2 a,b,c) and Myoma (2 d,e,f).

different levels of experience the subjective performance would probably have been worse.

Misdiagnosis in case of uterine sarcoma can indeed worsen the patient's prognosis if the lesion is morcellated [27–32]; similarly, a wrong classification of uterine myomas as uncertain or malignant could lead to an overtreatment (demolitive vs conservative surgery or surgery vs conservative management) of the patient.

In large retrospective studies, the rate of unexpected sarcoma in uterine specimens of women undergoing surgery for apparently benign disease ranged from 3 to 100 per 100,000 women [5,6].

Despite recent improvements in the accuracy of imaging techniques for gynecological malignancies, the differential diagnosis between myomas and uterine sarcomas remains a 'gray zone'.

In this scenario of uncertainty extremely dependent on US examiner subjective impression in the differential diagnosis of myometrial lesions, radiomics could represent an innovative and game-changer tool.

The main advantage of our model is that it does not depend on the experience of the US examiner, who only has to trace the contour basis of the lesion (then randomly modified by the software in order to avoid the operator dependence), export the images in DICOM format, send them to the TRACE4 platform, receiving a predictive classification of the mass in 'benign' or 'malignant' with an accuracy>80%.

According to our knowledge this is the first study that applies radiomics in accordance with IBSI guidelines and machine learning to US images in gynecology to differentiate benign from malignant myometrial tumors.

Similar experiences have been recently described in literature applied to ultrasound images in ovarian masses [13] and in hepatocellular carcinoma [33,34] where the authors concluded that radiomics could help in tumor evaluations, including diagnosis, differential diagnosis, and clinical prognosis.

The most important experiences in literature described radiomics applied to MRI, PET/CT or CT-scan; Xie et al. applied radiomics to MRI

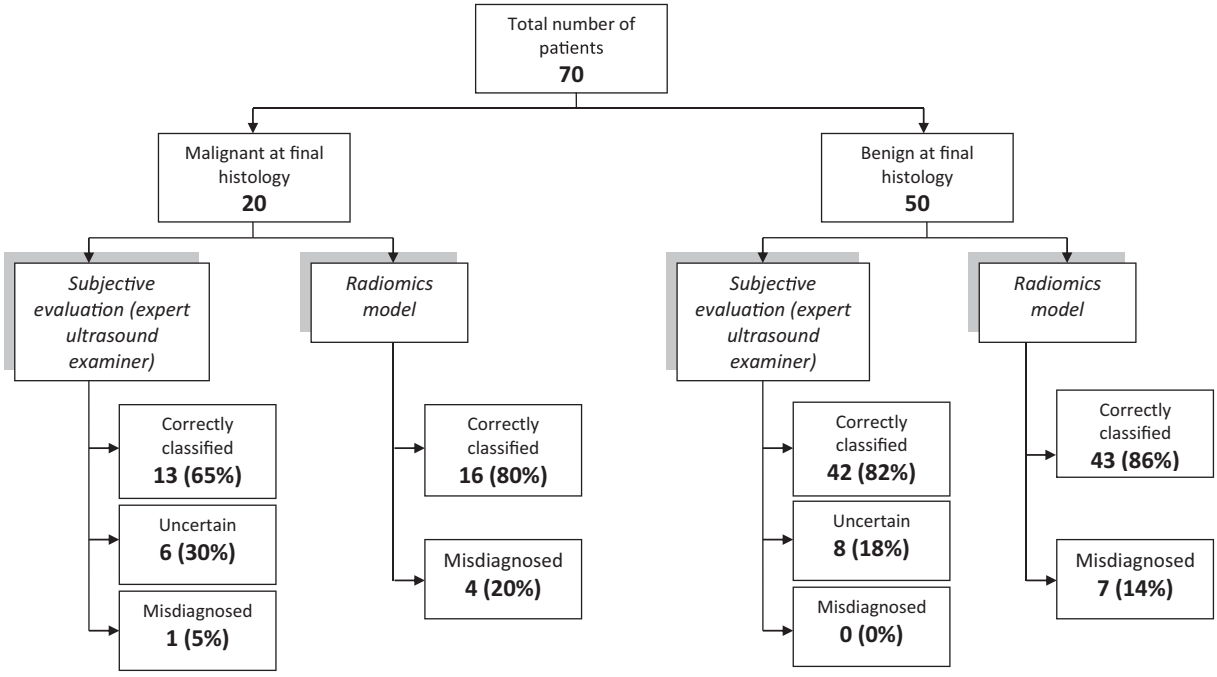

Fig. 3. Flow chart of the study.

images to discriminate between uterine sarcomas and myomas [35] in 78 women and they demonstrated that radiomic analysis was feasible and allowed results similar to those of an expert radiologist, thus being useful also as second expert reader.

A strength of our study is the supervision of the myometrial lesion by experienced ultrasound examiners from an oncological referral centre and the adoption of the radiomic analysis according to IBSI guidelines that allow better comparison with further analysis by other research groups. Moreover, we were able to use the final histological examination of all the myometrial lesions after surgery as gold standard for supervised training of the machine learning system.

However, the main weaknesses of the study is related to the inherit biases of the retrospective, single centre -study design and to the limited series sample size, but this is a pilot study to build a predictive model that will need to be further validated on larger series.

Declaration of Competing Interest

All Authors declare that they have no conflict of interest.

Appendix A. Supplementary data

Supplementary data to this article can be found online at https://doi.org/10.1016/j.ygyno.2021.04.004.

References

[1] E. D'Angelo, J. Prat, Uterine sarcomas: a review, Gynecol. Oncol. 116 (1) (2010 Jan) 131–139.
[2] F.J. Major, J.A. Blessing, S.G. Silverberg, C.P. Morrow, W.T. Creasman, J.L. Currie, E. Yordan, M.F. Brady, Prognostic factors in early-stage uterine sarcoma. A Gynecologic Oncology Group study, Cancer 71 (4 Suppl) (1993 Feb 15) 1702–1709.
[3] T. Hampton, Use of morcellation to remove fibroids scrutinized at FDA hearings, JAMA. 312 (6) (2014 Aug 13) 588.
[4] G. Bogani, V. Chiappa, A. Ditto, F. Martinelli, C. Donfrancesco, A. Indini, D. Lorusso, F. Raspagliesi, Morcellation of undiagnosed uterine sarcoma: a critical review, Crit Rev Oncol Hematol. 98 (2016 Feb) 302–308.
[5] S. Senapati, F.F. Tu, J.F. Magrina, Power morcellators: a review of current practice and assessment of risk, Am. J. Obstet. Gynecol. 212 (1) (2015 Jan) 18–23.
[6] I.S. Hagemann, A.R. Hagemann, V.A. LiVolsi, K.T. Montone, C.S. Chu, Risk of occult malignancy in morcellated hysterectomy: a case series, Int. J. Gynecol. Pathol. 30 (5) (2011 Sep) 476–483.
[7] G. Bogani, W.A. Cliby, G.D. Aletti, Impact of morcellation on survival outcomes of patients with unexpected uterine leiomyosarcoma: a systematic review and meta-analysis, Gynecol. Oncol. 137 (1) (2015 Apr) 167–172.
[8] J.D. Wright, A.I. Tergas, W.M. Burke, R.R. Cui, C.V. Ananth, L. Chen, D.L. Hershman, Uterine pathology in women undergoing minimally invasive hysterectomy using morcellation, JAMA. 312 (12) (2014 Sep 24) 1253–1255.
[9] S. Nougaret, H. Tibermacine, M. Tardieu, E. Sala, Radiomics: an introductory guide to what it may foretell, Curr. Oncol. Rep. 21 (8) (2019 Jun 25) 70.
[10] D. Kumbhare, S. Shaw, S. Ahmed, M.D. Noseworthy, Quantitative ultrasound of trapezius muscle involvement in myofascial pain: comparison of clinical and healthy population using texture analysis, J Ultrasound. 23 (1) (2020 Mar) 23–30.
[11] A.C. Yeh, H. Li, Y. Zhu, J. Zhang, G. Khramtsova, K. Drukker, A. Edwards, S. McGregor, T. Yoshimatsu, Y. Zheng, Q. Niu, H. Abe, J. Mueller, S. Conzen, Y. Ji, M.L. Giger, O.I. Olopade, Radiogenomics of breast cancer using dynamic contrast enhanced MRI and gene expression profiling, Cancer Imaging 19 (1) (2019 Jul 15) 48.
[12] M.A. Mazurowski, Radiogenomics: what it is and why it is important, J. Am. Coll. Radiol. 12 (8) (2015 Aug) 862–866.
[13] V. Chiappa, G. Bogani, M. Interlenghi, C. Salvatore, F. Bertolina, G. Sarpietro, M. Signorelli, I. Castiglioni, F. Raspagliesi, The Adoption of Radiomics and machine learning improves the diagnostic processes of women with Ovarian MAsses (the AROMA pilot study), J Ultrasound. (2020 Jul 21) https://doi.org/10.1007/s40477-020-00503-5 (Epub ahead of print).
[14] H.J. Aerts, E.R. Velazquez, R.T. Leijenaar, C. Parmar, P. Grossmann, S. Carvalho, J. Bussink, R. Monshouwer, B. Haibe-Kains, D. Rietveld, F. Hoebers, M.M. Rietbergen, C.R. Leemans, A. Dekker, J. Quackenbush, R.J. Gillies, P. Lambin, Decoding tumour phenotype by noninvasive imaging using a quantitative radiomics approach, Nat. Commun. 5 (2014 Jun 3) 4006.
[15] M. Ludovisi, F. Moro, T. Pasciuto, S. Di Noi, S. Giunchi, L. Savelli, M.A. Pascual, P. Sladkevicius, J.L. Alcazar, D. Franchi, R. Mancari, M.C. Moruzzi, D. Jurkovic, V. Chiappa, S. Guerriero, C. Exacoustos, E. Epstein, F. Frühauf, D. Fischerova, R. Fruscio, F. Ciccarone, G.F. Zannoni, G. Scambia, L. Valentin, A.C. Testa, Imaging in gynecological disease (15): clinical and ultrasound characteristics of uterine sarcoma, Ultrasound Obstet. Gynecol. 54 (5) (2019 Nov) 676–687.
[16] D. Timmerman, L. Valentin, T.H. Bourne, W.P. Collins, H. Verrelst, I. Vergote, International Ovarian Tumor Analysis (IOTA) Group. Terms, definitions and measurements to describe the sonographic features of adnexal tumors: a consensus opinion from the International Ovarian Tumor Analysis (IOTA) Group, Ultrasound Obstet. Gynecol. 16 (5) (2000 Oct) 500–505.
[17] T. Van den Bosch, M. Dueholm, F.P. Leone, L. Valentin, C.K. Rasmussen, A. Votino, D. Van Schoubroeck, C. Landolfo, A.J. Installé, S. Guerriero, C. Exacoustos, S. Gordts, B. Benacerraf, T. D'Hooghe, B. De Moor, H. Brölmann, S. Goldstein, E. Epstein, T. Bourne, D. Timmerman, Terms, definitions and measurements to describe sonographic features of myometrium and uterine masses: a consensus opinion from the Morphological Uterus Sonographic Assessment (MUSA) group, Ultrasound Obstet. Gynecol. 46 (3) (2015 Sep) 284–298.
[18] J. Prat, FIGO staging for uterine sarcomas, Int. J. Gynaecol. Obstet. 104 (3) (2009 Mar) 177–178.
[19] R.J. Kurman, M.L. Carcangiu, C.S. Herrington, R.H. Young (Eds.), WHO Classification of Tumours of Female Reproductive Organs, 4th ed.WHO, Geneva, 2014.
[20] A. Zwanenburg, S. Leger, M. Valli'eres, S. Lock, Image biomarker standardisation initiative, arXiv: Computer Vision and Pattern Recognition (2016) (arXiv:1612.07003).
[21] Ronald L. Wasserstein, Nicole A. Lazar, The ASA statement on p-values: context, process, and purpose, Am. Stat. 70 (2) (2016) 129–133.
[22] K. Hajian-Tilaki, Sample size estimation in diagnostic test studies of biomedical informatics, J. Biomed. Inform. 48 (2014) 193–204, https://doi.org/10.1016/j.jbi.2014.02.013.
[23] K.C. Wen, H.C. Horng, P.H. Wang, Y.J. Chen, M.S. Yen, H.T. Ng, Taiwan Association of Gynecology Systematic Review Group, Uterine sarcoma part I – uterine leiomyosarcoma: the topic advisory group systematic review, Taiwan J Obstet Gynecol 55 (2016) 463–471.
[24] C. Exacoustos, M.E. Romanini, A. Amadio, C. Amoroso, B. Szabolcs, E. Zupi, D. Arduini, Can gray-scale and color Doppler sonography differentiate between uterine leiomyosarcoma and leiomyoma? J. Clin. Ultrasound 35 (8) (2007 Oct) 449–457.
[25] M.A. Kliewer, B.S. Hertzberg, P.Y. George, J.W. McDonald, J.D. Bowie, B.A. Carroll, Acoustic shadowing from uterine leiomyomas: sonographic– pathologic correlation, Radiology 196 (1995) 99–102.
[26] M. Dueholm, Transvaginal ultrasound for diagnosis of adenomyosis: a review, Best Pract Res Clin Obstet Gynaecol 20 (2006) 569–582.
[27] B.A. Goff, SGO not soft on morcellation: risks and benefits must be weighed, Lancet Oncol. 15 (4) (2014 Apr), e148.
[28] J.Y. Park, S.K. Park, D.Y. Kim, J.H. Kim, Y.M. Kim, Y.T. Kim, J.H. Nam, The impact of tumor morcellation during surgery on the prognosis of patients with apparently early uterine leiomyosarcoma, Gyn Onc 122 (2) (2011) 255–259.
[29] S. George, C. Barysauskas, C. Serrano, T. Oduyebo, J.A. Rauh-Hain, M.G. Del Carmen, G.D. Demetri, M.G. Muto, Retrospective cohort study evaluating the impact of intraperitoneal morcellation on outcomes of localized uterine leiomyosarcoma, Cancer. 120 (20) (2014 Oct 15) 3154–3158.
[30] M. Lieng, E. Berner, B. Busund, Risk of morcellation of uterine leiomyosarcomas in laparoscopic supracervical hysterectomy and laparoscopic myomectomy, a retrospective trial including 4791 women, J. Minim. Invasive Gynecol. 22 (3) (2015 Mar-Apr) 410–414.
[31] R. Ton, G.S. Kilic, J.Y. Phelps, A medical-legal review of power morcellation in the face of the recent FDA warning and litigation, J. Minim. Invasive Gynecol. 22 (4) (2015 May-Jun) 564–572.
[32] E.A. Pritts, W.H. Parker, J. Brown, D.L. Olive, Outcome of occult uterine leiomyosarcoma after surgery for presumed uterine fibroids: a systematic review, J. Minim. Invasive Gynecol. 22 (1) (2015 Jan) 26–33.
[33] Z. Yao, Y. Dong, G. Wu, Q. Zhang, D. Yang, J.H. Yu, W.P. Wang, Preoperative diagnosis and prediction of hepatocellular carcinoma: Radiomics analysis based on multimodal ultrasound images, BMC Cancer 18 (1) (2018 Nov 12) 1089.
[34] H.T. Hu, Z. Wang, X.W. Huang, S.L. Chen, X. Zheng, S.M. Ruan, X.Y. Xie, M.D. Lu, J. Yu, J. Tian, P. Liang, W. Wang, M. Kuang, Ultrasound-based radiomics score: a potential biomarker for the prediction of microvascular invasion in hepatocellular carcinoma, Eur. Radiol. 29 (6) (2019 Jun) 2890–2901.
[35] H. Xie, J. Hu, X. Zhang, S. Ma, Y. Liu, X. Wang, Preliminary utilization of radiomics in differentiating uterine sarcoma from atypical leiomyoma: comparison on diagnostic efficacy of MRI features and radiomic features, Eur. J. Radiol. 115 (2019 Jun) 39–45.